HHS Public Access

Author manuscript

Acta Neuropathol. Author manuscript; available in PMC 2017 December 01.

Published in final edited form as:

Acta Neuropathol. 2016 December ; 132(6): 931–933. doi:10.1007/s00401-016-1618-1.

[18F]AV-1451 tau-PET uptake does correlate with quantitatively measured 4R-tau burden in autopsy confirmed corticobasal degeneration

Keith A. Josephs, MD, MST, MSc[¥], **Jennifer L. Whitwell, PhD**[‡], **Pawel Tacik, PhD**[†], **Joseph R. Duffy, PhD**[¥], **Matthew L. Senjem, MS**[π], **Nirubol Tosakulwong, BS**[≠], **Clifford R. Jack Jr, MD**[‡], **Val Lowe, MD**[‡], **Dennis W. Dickson, MD**[†], and **Melissa E. Murray, PhD**[†]

[¥]Department of Neurology, Mayo Clinic, Rochester MN

[‡]Department of Radiology, Mayo Clinic, Rochester MN

[π]Department of Information Technology, Mayo Clinic, Rochester MN

[≠]Health Sciences Research, Mayo Clinic, Rochester MN

[†]Department of Neuroscience, Mayo Clinic, Jacksonville Florida

Corticobasal degeneration (CBD) is a neurodegenerative disease characterized by the deposition of abnormally hyperphosphorylated 4-repeat (4R) tau in the brain[3]. Recent advances in molecular neuroimaging include the production of positron emission tomography (PET) ligands that bind to abnormal tau in the brain. One such ligand, [18F]AV-1451, has been shown to bind to abnormal 3R+4R tau in diseases such as Alzheimer's disease[2]. In addition, one case report found an association between antemortem [18F]AV-1451 and tau burden in an autopsied case with a mutation in the microtubule-associated protein tau gene with 3R+4R tau[9]. Autoradiographic studies however have found very little, if any, binding in diseases characterized by 4R-tau including CBD[6–8], and no PET-autopsy studies have been published for a 4R-tau disease.

We assessed the relationship between [18F]AV-1451 uptake on PET with tau burden at autopsy, and with measures of neurodegeneration from [18F]fluorodeoxyglucose (FDG) PET and MRI, in a patient with autopsy-confirmed CBD as well as performed correlative autoradiography, as previously described[6]. The male patient died aged 59 after a 10-year history of progressive neurological decline. He first presented with difficulty getting his words out and was diagnosed with primary progressive apraxia of speech[5]. Over time, he developed difficulty with language, swallowing difficulties, ideomotor apraxia, marked parkinsonism, and balance and gait problems, (Online resource 1) hence his clinical diagnosis was later changed to corticobasal syndrome[1]. He tested negative for microtubule-associated protein tau mutations. Autopsy revealed 4R tau-positive, but 3R tau-negative threads in grey and white matter of cortex, basal ganglia, thalamus and brainstem, as well as pretangles, astrocytic plaques and coiled bodies (oligodendroglial inclusions)

Corresponding Author: Keith A. Josephs, MD, MST, MSc, Professor and Consultant of Neurology, Divisions of Behavioral Neurology & Movement Disorders, Mayo Clinic, Rochester, MN 55905, Tele: (507)-538-1038, Fax: (507)-538-6012, josephs.keith@mayo.edu.

consistent with a diagnosis of CBD[3] (Fig. 1A, Online Resource 1). Fourteen months prior to death, he underwent [18F]AV-1451 PET, as well as Pittsburgh-compound B (PiB) PET, FDG-PET and a 3T volumetric MRI. In addition, he had undergone MRI scans 9-months and 22-months before death.

We abstracted tau burden at autopsy, tau-PET uptake, FDG-PET uptake, grey matter volumes and grey matter rates of atrophy for the identical set of 10 regions-of-interest (ROIs) in the left hemisphere (middle frontal, supplementary motor area, primary motor, Broca's area, orbitofrontal cortex, inferior parietal, superior temporal, parahippocampal gyrus, visual cortex and striatum). Tau burden at autopsy was determined quantitatively. All 10 ROIs were scanned at ultra-resolution on the ScanScopeXT from which large areas of interest were annotated using ImageScope-11.2 (Aperio Technologies, Vista, CA). Annotated regions were analyzed in Spectrum-11.2 using a custom-designed color deconvolution algorithm to detect only abnormal tau[4] (Fig. 1a). Tau burden was expressed as the area of immunoreactive pixels to the total area of the annotated region. The automated anatomical labeling atlas was used to output ROI data from neuroimaging (Online Resource 2). To create standard uptake ratios (SUVRs), tau-PET uptake in each ROI was divided by uptake in cerebellar crus grey matter, and FDG-PET uptake was divided by uptake in pons. Grey matter volumes were divided by total intracranial volume and were expressed as z-scores representing difference from 10 cognitively-normal male controls that were the same age as our patient. In addition, annualized regional rates of atrophy were calculated using tensor-based morphometry using the serial scans that straddled the time of the tau-PET scan, i.e. those performed 9 and 22 months before death (Online Resource 2). Spearman rank correlations were calculated using JMP software (JMP Software, version 10.0.0; SAS Institute Inc, Cary, NC) with α=0.05.

Tau-PET revealed increased signal in putamen, pallidum, thalamus, precentral cortex, rolandic operculum, supplemental motor area, and left Broca's area (Fig. 2). The PiB-PET scan was negative (Fig. 2) (global PiB SUVR=1.28). Regional tau-PET SUVR values strongly correlated with autopsy tau burden across the 10 ROIs (r=0.89, p=0.0005) (Fig. 1c). Tau-PET SUVRs showed non-significant correlations with FDG-PET (r=-0.50, p=0.14), grey matter volume (r=−0.43, p=0.21) and rates of atrophy (r=−0.43, p=0.21) (Fig. 1c). [18F]AV-1451 autoradiography revealed minimal, displaceable binding in areas where dense 4R tau deposition was observed on immunohistochemistry (Fig. 1b).

Regional [18F]AV-1451 uptake showed an excellent correlation with underlying, quantitatively measured, 4R-tau burden in our case, that did not appear to be driven by neurodegeneration. With-that said, there does appear to be a disconnect between antemortem and postmortem binding to 4R tau pathology. Furthermore, our correlative autoradiographic study reveals that the ligand may be binding only a very small fraction of the total 4R-tau burden. More work is therefore needed to better understand the relationship between [18F]AV-1451 and 4R tau, and to determine whether [18F]AV-1451 could be a disease biomarker to study CBD.

Supplementary Material

Refer to Web version on PubMed Central for supplementary material.

Acknowledgments

This study was supported by NIH grants R01-NS89757 (PI, Josephs) and R01-DC12519 (PI, Whitwell)

References

1. Armstrong MJ, Litvan I, Lang AE, et al. Criteria for the diagnosis of corticobasal degeneration. Neurology. 2013; 80:496–503. DOI: 10.1212/WNL.0b013e31827f0fd1 [PubMed: 23359374]
2. Chien DT, Bahri S, Szardenings AK, et al. Early clinical PET imaging results with the novel PHF-tau radioligand [F-18]-T807. J Alzheimers Dis. 2013; 34:457–468. DOI: 10.3233/JAD-122059 [PubMed: 23234879]
3. Dickson DW, Bergeron C, Chin SS, et al. Office of Rare Diseases neuropathologic criteria for corticobasal degeneration. J Neuropathol Exp Neurol. 2002; 61:935–946. [PubMed: 12430710]
4. Josephs KA, Whitwell JL, Ahmed Z, et al. Beta-amyloid burden is not associated with rates of brain atrophy. Ann Neurol. 2008; 63:204–212. DOI: 10.1002/ana.21223 [PubMed: 17894374]
5. Josephs KA, Duffy JR, Strand EA, et al. Characterizing a neurodegenerative syndrome: primary progressive apraxia of speech. Brain. 2012; 135:1522–1536. DOI: 10.1093/brain/aws032 [PubMed: 22382356]
6. Lowe VJ, Curran G, Fang P, et al. An autoradiographic evaluation of AV-1451 Tau PET in dementia. Acta Neuropathol Commun. 2016; 4:58.doi: 10.1186/s40478-016-0315-6 [PubMed: 27296779]
7. Marquie M, Normandin MD, Vanderburg CR, et al. Validating novel tau positron emission tomography tracer [F-18]-AV-1451 (T807) on postmortem brain tissue. Ann Neurol. 2015; 78:787–800. DOI: 10.1002/ana.24517 [PubMed: 26344059]
8. Sander K, Lashley T, Gami P, et al. Characterization of tau positron emission tomography tracer [F]AV-1451 binding to postmortem tissue in Alzheimer's disease, primary tauopathies, and other dementias. Alzheimers Dement. 2016; doi: 10.1016/j.jalz.2016.01.003
9. Smith R, Puschmann A, Scholl M, et al. 18F-AV-1451 tau PET imaging correlates strongly with tau neuropathology in MAPT mutation carriers. Brain. 2016; 139:2372–2379. DOI: 10.1093/brain/aww163 [PubMed: 27357347]

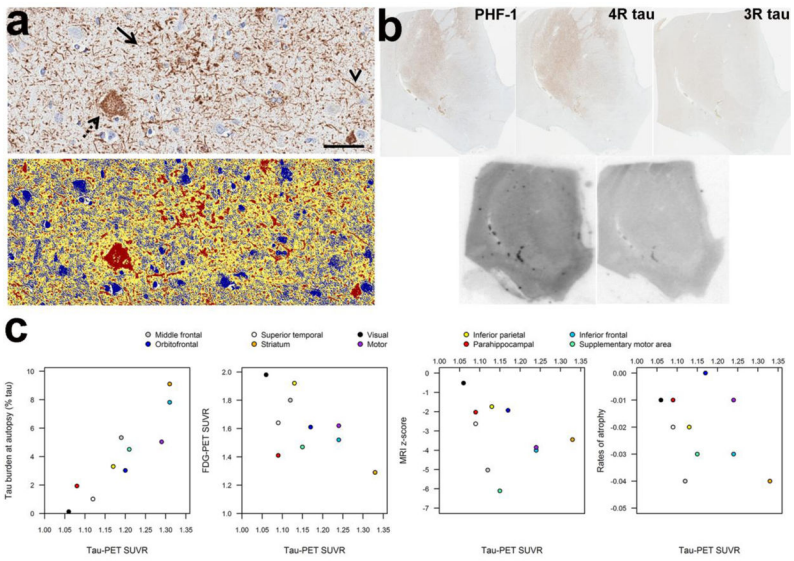

Fig. 1.

Autopsy findings (a), autoradiography (b) and scatter-plots showing the relationship between tau-PET SUVR and tau burden at autopsy, as well as other measures of neurodegeneration (c). **Panel a** shows the tau burden assessment in our patient with CBD. Top image shows the tau immunostained tissue (CP13, mouse IgG1, 1:1000, Peter Davies, Albert Einstein College of Medicine, Bronx, NY), with the bottom image showing the custom-designed color deconvolution algorithm to highlight tau deposition (shown in red). Characteristic astrocytic plaques (arrow), ballooned neurons (dashed arrow), and thread-like processes (arrowhead) were observed and quantified. (Scale bar = 50 μm). Images shown are from inferior frontal cortex. **Panel b** shows tau immunohistochemistry and correlative autoradiography. Top row shows tau immunohistochemistry with PHF-1(1:1000 mouse monoclonal anti-phospho-serine 396/404 tau, gift from Peter Davies), 4R tau and 3R tau (RD4 and RD3, mouse IgG, Millipore, Temecula, CA) going from left to right (note 3R tau staining was negative) and bottom row shows [18F]AV-1451 autoradiography and [18F]AV-1451 blocked autoradiography in the nucleus accumbens. There was minimal, displaceable [18F]AV-1451 autoradiography binding corresponding to regions where 4R burden was most dense on immunohistochemistry. **Panel c** shows scatter-plots of the relationship between tau-PET SUVR and tau burden at autopsy, FDG-PET SUVR, MRI z-scores, and MRI rates of atrophy. The tau-PET data used in the correlation with tau burden at autopsy was calculated over grey and white matter within the ROI, whereas the tau-PET data used in the imaging plots was calculated over grey matter only to match the FDG and MRI data.

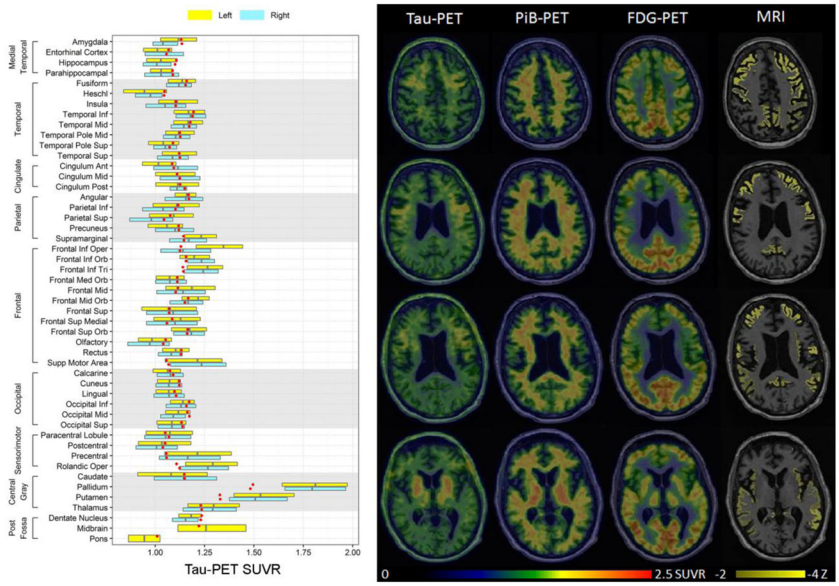

Fig. 2.

Tau-PET, PiB-PET, FDG-PET and MRI from our CBD patient. The tau-PET findings are shown on representative axial slices through the brain and in a box-plot showing regional SUVR values for the left and right hemisphere. Regional values were generated using the automated anatomical labeling atlas, with boxes representing median, 25th and 75th percentile values across all the voxels in each region. The red dots represent the median tau-PET SUVRs from a group of controls matched by age and gender to our patient. Tau-PET revealed increased signal in the putamen, pallidum, thalamus, precentral cortex, rolandic operculum, supplemental motor area, and left Broca's area (frontal inferior opercular and frontal inferior triangularis). The PiB-PET, FDG-PET and MRI scans are also shown on representative axial slices. The three PET scans are shown on the same color scale while MRI scan highlights regions with z-scores between -2 and -4 standard deviations from controls. No increased signal was observed on PiB-PET. The FDG-PET revealed hypometabolism in the caudate nucleus, insula and throughout the posterior frontal lobes, including medial and lateral premotor and primary motor cortices, with greater abnormalities observed in the left hemisphere. The MRI showed more widespread abnormalities throughout the brain, although the most severe atrophy was observed in the frontal lobe. Inf = inferior, Mid = middle, Sup = superior, Ant = anterior, Post = posterior, Orb = orbital, Tri = triangularis.